Tectonic influence of multi-ring basins:
The case of Mercury's Discovery Quadrangle and the Andal-Coleridge basin

A. Sepe[1,2], L. Ferranti[2,1], V. Galluzzi[1], G. W. Schmidt[1], S. Buoninfante[2,1], and P. Palumbo[1]

[1] INAF, Institute for Space Astrophysics and Planetology (IAPS), Rome, Italy (antonio.sepe@inaf.it)
[2] University of Naples "*Federico II*", Department of Earth Sciences, Environment and Resources, Naples, Italy

EUROPLANET SCIENCE CONGRESS EPSC2024

Introduction

Mercury's Discovery quadrangle (H-11), located at southern mid-latitudes (22.5°S-65°S and 270°E-360°E, Fig.1), is thought to host a **pre-Tolstojan multi-ring impact basin** named **Andal–Coleridge**, probably surrounded by a three- to five-ring system [1,2].

Main Purposes

By using NASA/MESSENGER end-of-mission products [3] we produced a high-resolution structural map of the quadrangle to support the production of the 1:3M-scale geologic map by [4], and perform a structural analysis to validate and ascertain the existence of the Andal-Coleridge basin and investigate its influence on the tectonic evolution of this region.

1. Structural Framework

Our structural map (Fig.1) shows ~500 segments of compressive features (lobate scarps, high-relief ridges and wrinkle ridges) mainly arranged in a **circular pattern** at the approximate centre of the quadrangle, encircling both a broad **topographic low** and a **mascon-like feature** (Fig.2).
The general uniform distribution of bins shown in rose diagrams suggests an **impact-related nature** for most structures [5].

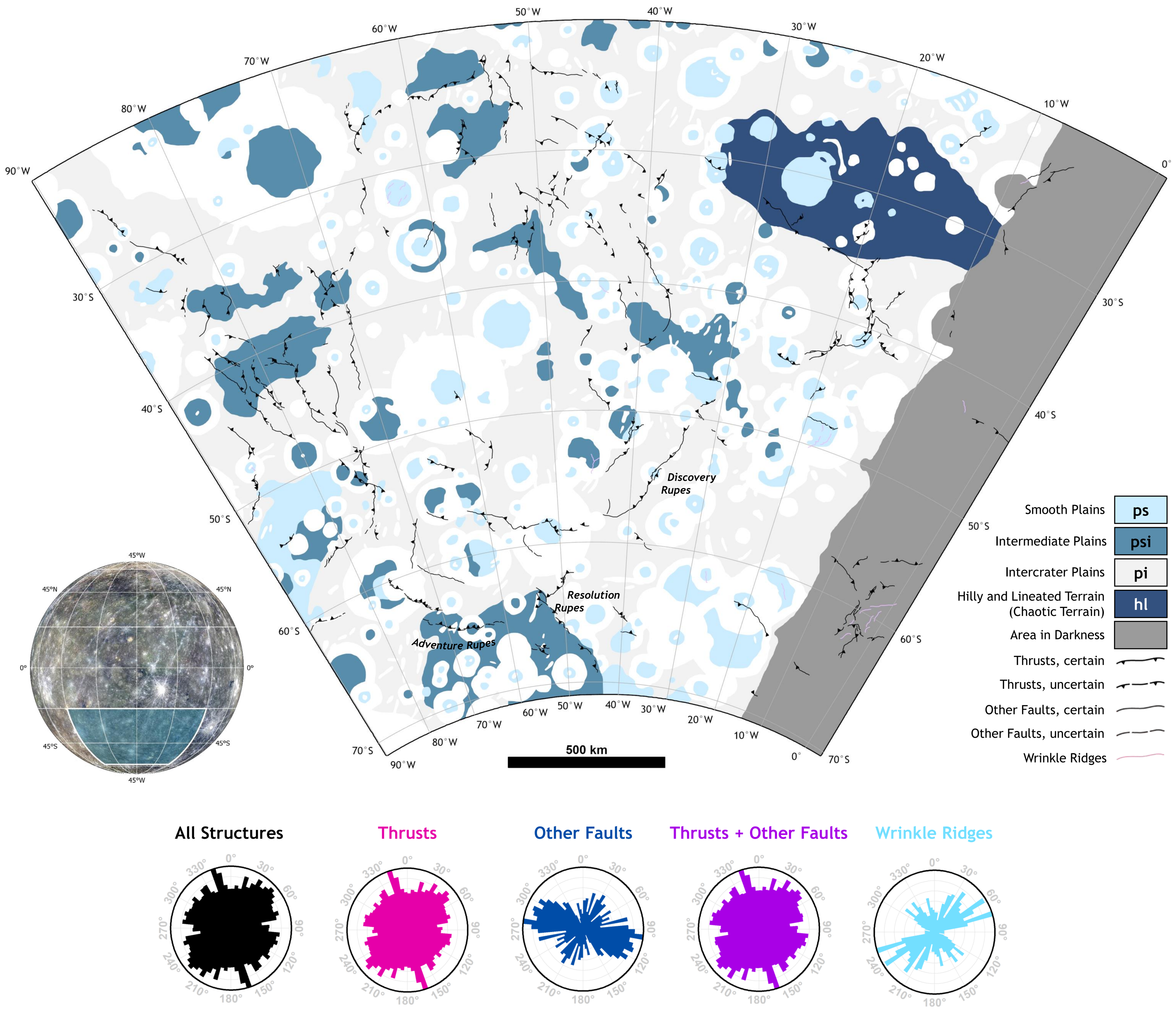

Figure 1 Structural map of the Discovery quadrangle overlayed to a simplified version of the geologic map of [6]. We used Mariner10 boundaries for this quadrangle in order to include the Adventure Rupes since it partially lies in the Bach quadrangle (H-15).

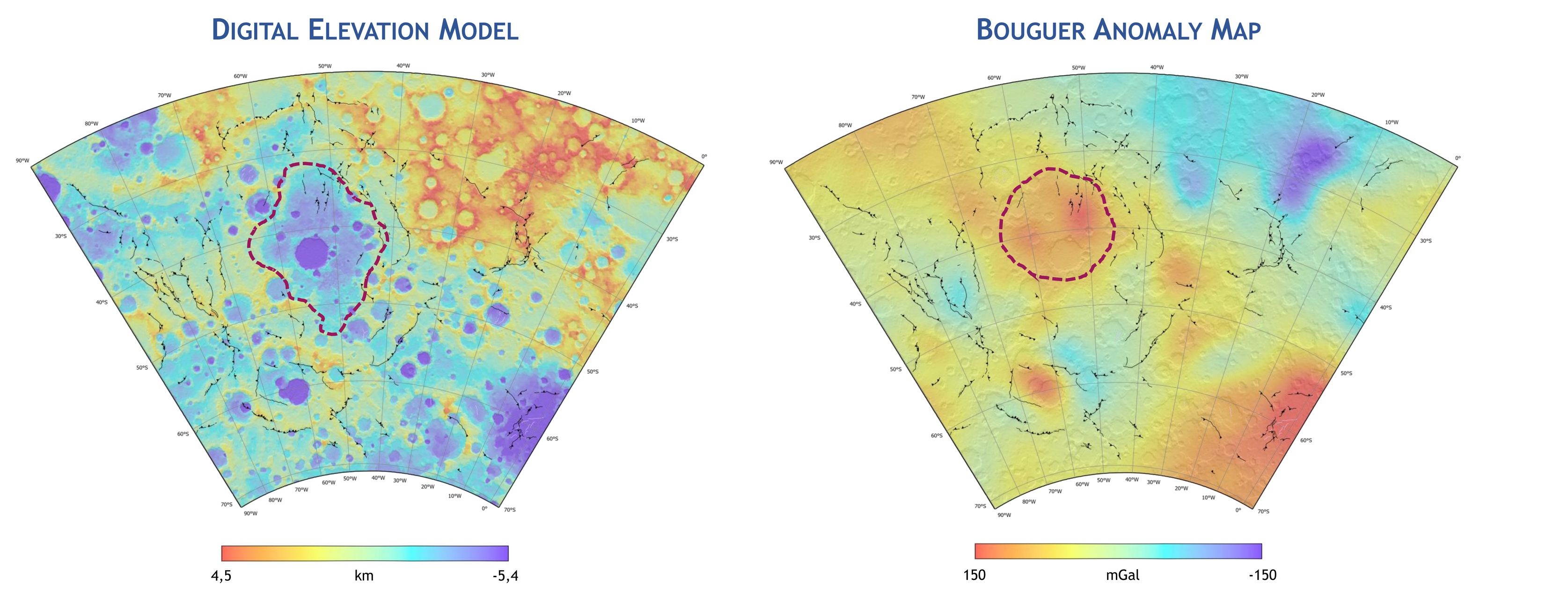

Figure 2 Structural map of the Discovery quadrangle overlayed to the Digital Elevation Model of [7] (left) and the Bouguer Anomaly Map of [8] (right). The red dashed line approximately delimits the topographic low and the mascon-like feature respectively.

2. Beta-Analysis

The beta-analysis [9] results in a bimodal distribution of intersections (Fig.3), suggesting the presence of two distinct basins: the **Andal-Coleridge basin** and the informally named **b78 basin** [10]. **Discovery Rupes** is part of the Andal-Coleridge-bounding faults. **Adventure** and **Resolution Rupes** are part of the b78-bounding faults.

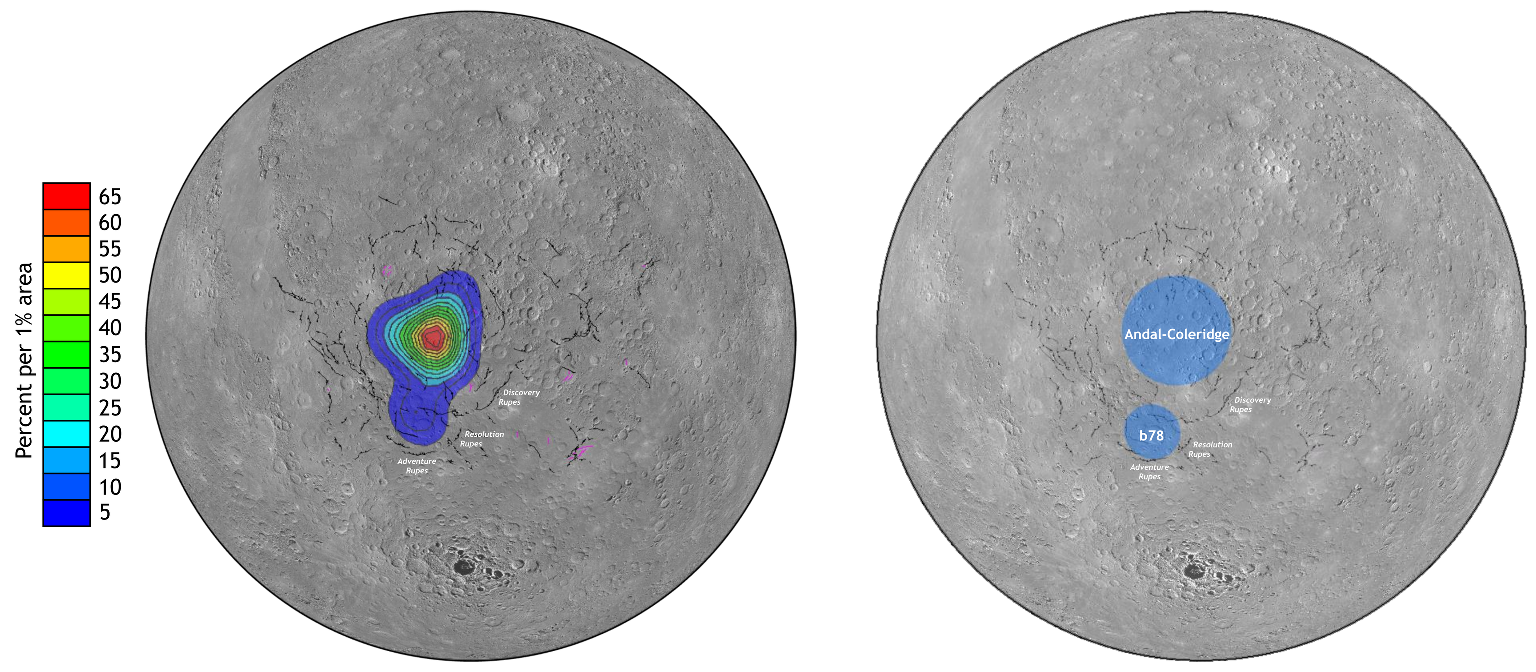

Figure 3 (left) The distribution of intersections resulting from beta-analysis in stereographic projection centred at quadrangle's centre and overlayed to the BDR Global Basemap. The maximum density of intersections (65%) is approximately located at 54.3°W, 45°S. (right) The hypothesised location and extent of Andal-Coleridge and b78 basins from [10] centred respectively in 41.1°W, 51.2°S and 60°W, 62.7°S.

3. Throw-Height Analysis

The throw-height analysis (Fig.4) confirms that **Discovery**, **Adventure** and **Resolution scarps** are the morphological expression of two different faults [1]: the **Discovery fault** bounds the Andal-Coleridge basin while the **Adventure-Resolution fault** bounds the b78 basin. These faults grew **hard-linking** several segments together defining a **growth-fault system (DAR system)**, since the cumulative throw falls approximately at the centre of the system, consistent with terrestrial fault growth patterns [e.g. 11].
Discovery Rupes shows evidences of reactivation within **Rameau crater.** Adopting previous dating of Rameau crater and Discovery Rupes [12,13], we propose a preliminary chronology for the evolution of the Discovery Rupes (Fig.5).

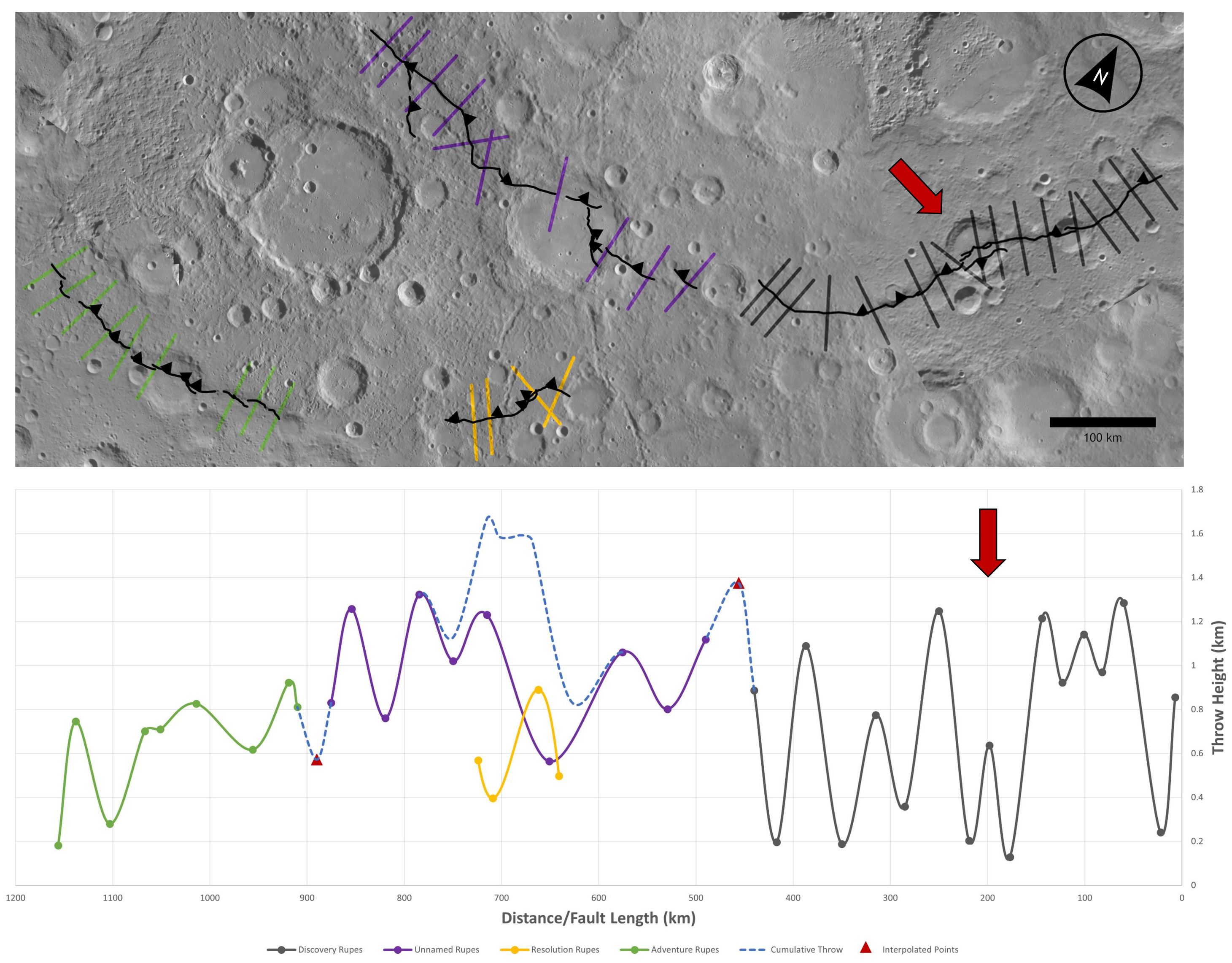

Figure 4 (top) The DAR system and the 40 profiles used to produce the throw-height profile. (bottom) The throw-height profile of the DAR system. Each peak represents a single fault segment. Red arrows indicate the location of Rameau crater.

Figure 5

Andal-Coleridge Impact Event
pre-Tolstojan

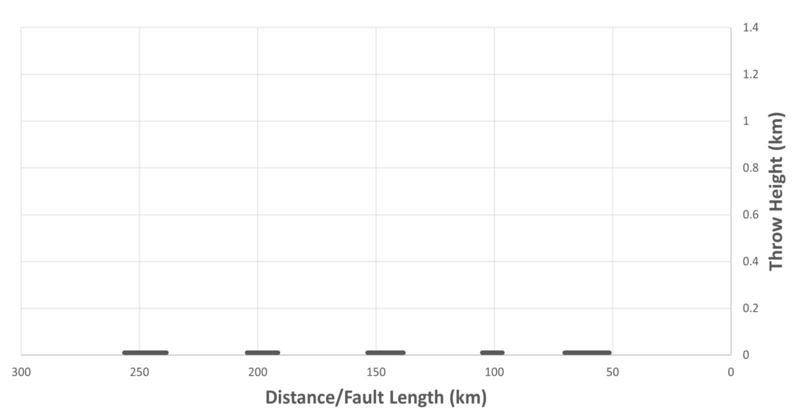

During pre-Tolstojan (>4 Gya) the Andal-Coleridge impact event occurred generating a system of basin-related fractures.

Global Contraction
Tolstojan

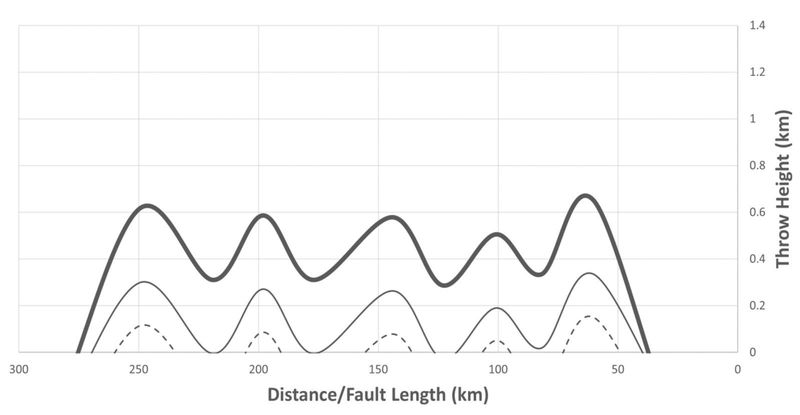

Mercury's global contraction caused the growth (thin dashed line) and the linking (solid thin line) of the fractures into longer and higher faults (**solid thick line**).

Rameau Crater Formation
Tolstojan

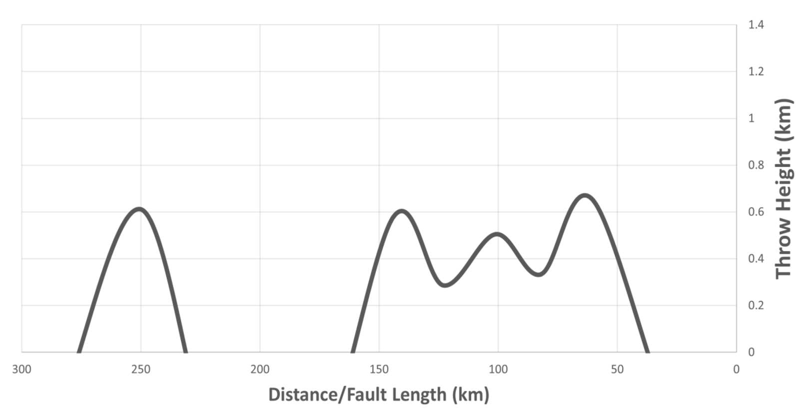

During the Tolstojan period (4–3.85 Gya) the Rameau-forming impact event occurred eroding locally the surficial trace of Discovery Rupes.

Global Contraction
Tolstojan-Mansurian/Present Day

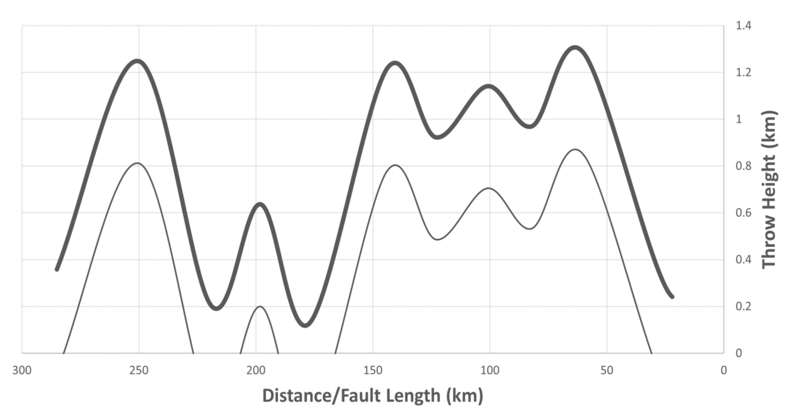

The global contraction allowed both the throw accumulation on the preserved fault-trace and the reactivation of the eroded segment within Rameau crater (thin line) up to Mansurian/Present day (<1.7 Gya) (**thick line**).

Conclusions and Future Work

The tectonics of Discovery quadrangle has been significantly influenced by the Andal-Coleridge and b78 impact basins. These impact events created mechanical discontinuities in the crust, which later connected to form linked fault-systems due to Mercury's global contraction. The effect of the global contraction is evident within Rameu crater, where Discovery Rupes exhibits signs of post-impact reactivation. Our preliminary analysis indicates that throw rates peaked during the Tolstojan period, declined through the Mansurian period, and may continue to the present day [14].

Our study supports the hypothesis that ancient basins played a key role in the localization and orientation of faults, shaping the structural framework that accommodated the global contraction [15].
We aim at enhancing the structural analysis of the quadrangle to better understand the nature of the NW-SE-trending structures, probably related to the high-magnesium region as observed in other quadrangles [16]. This study also aims at contributing to the evaluation of the rate and magnitude of Mercury's global contraction throughout its geological history.

References

[1] Watters et al. (2001). Plan. and Sp. Sci., 49(14-15), 1523-1530. [2] Spudis and Strobell (1984). LPSC, 814-815. [3] Denevi et al. (2017). Sp. Sci. Rev., 214(1). [4] Blance et al. (2023). LPSC Contrib. No. 2806. [5] Delbo et al. (2019). LPI Contrib. No. 2189. [6] Trask and Dzurisin (1984). USGS, IMAP 1658. [7] Becker et al. (2016). LPSC Contrib. No. 1903. [8] Buoninfante et al. (2023). Sci. Rep., 13, 19854. [9] Anderson et al. (2001). JGR: Planets, 106(E9), 20563-20585. [10] Orgel et al. (2020). JGR: Planets, 125(8). [11] Kim and Sanderson (2005). Earth-Sci. Rev., 68(3-4), 317-334. [12] Kinczyk et al. (2020). Icarus, 341, 113637. [13] Clark et al. (2024). LPSC Contrib. No. 3040. [14] Tosi et al. (2013). JGR: Planets, 118(12), 2474-2487. [15] Spudis and Guest (1988). In: Vilas, F., Chapman, C.R., Matthews, M.S. (Eds.), Mercury, 137-159. [16] Galluzzi et al. (2019). JGR: Planets, 124(10), 2543-2562.

~ We gratefully acknowledge funding from the Italian Space Agency (ASI) under ASI-INAF agreement 2017-47-H1 ~